Plane Wave Radial Filter Design Using Pre-emphasized Time-Domain Representations

Nara Hahn[1,2], Frank Schultz[2], and Sascha Spors[2]

[1] *Institute of Sound and Vibration Research, University of Southampton, Southampton, UK*

[2] *Institute of Communications Engineering, University of Rostock, Rostock, Germany*

Email: nara.hahn@soton.ac.uk

Introduction

Spherical harmonic representations are commonly used in spatial sound field capture, processing, and reproduction [1, 2, 3, 4]. The angular/directional dependency of the individual modes is described by the spherical harmonics or the Legendre functions whereas the radial dependency by the spherical Bessel/Hankel functions. In practice, the radially dependent components are realized as digital filters (so-called *radial filters*) which model the spatiotemporal and spectral properties of each mode [5, 6, 7, 8]. This paper addresses the design of radial filters modeling the sound field of a plane wave. The filter coefficients are derived analytically based on the time-domain expressions of the modal impulse responses. As outlined in the following section, the presented approach can be considered as a computationally efficient alternative to the existing methods [9, 10].

Plane Wave Radial Filters

Let us assume a plane wave propagating in the direction $\boldsymbol{n}_{\mathrm{pw}} = (1, \theta_{\mathrm{pw}}, \phi_{\mathrm{pw}})$ with θ_{pw} and ϕ_{pw} respectively denoting the colatitude and azimuth angle. The spherical harmonic expansion of the plane wave reads [1, Eq. (6.175)]

$$e^{-i\frac{\omega}{c}r\cos\Theta} = \sum_{n=0}^{\infty}(2n+1)i^{-n}j_n(\tfrac{\omega}{c}r)P_n(\cos\Theta) \qquad (1)$$

in the frequency domain[1], and [11, Eq. (11)]

$$\delta\big(t-\tfrac{r}{c}\cos\Theta\big) = \begin{cases} 0, & |\frac{c}{r}t| > 1 \\ \sum_{n=0}^{\infty}(2n+1)\frac{c}{2r}P_n(\frac{c}{r}t)P_n(\cos\Theta), & |\frac{c}{r}t| < 1 \end{cases} \qquad (2)$$

in the time domain. The modal transfer functions are described by the spherical Bessel functions $j_n(\frac{\omega}{c}r)$, whereas the finite-length modal impulse responses by the Legendre polynomials $P_n(\frac{c}{r}t)$. The directivity of each mode is represented by $P_n(\cos\Theta)$ where Θ is the angle between $\boldsymbol{n}_{\mathrm{pw}}$ and the evaluation point $\boldsymbol{x} = (r, \theta, \phi)$ with r denoting the radius, θ the colatitude, and ϕ the azimuth.

The modal impulse responses and transfer functions are depicted in the first row (blue) of Fig 1(a) and 1(b), respectively. Note that the transfer functions exhibit nth-order zero(s) at $\omega = 0$, which will be relevant when we apply the pre-emphasis in the following. The finite support ($|\frac{c}{r}t| < 1$) of the modal impulse response suggests that the radial functions can be modeled by a finite impulse response (FIR) filter in a discrete-time system.

However, designing the FIR radial filter based on the time-domain expression (2) is not trivial. Note from Fig. 1(b) that the modal spectrum (blue) is not band-limited in the temporal frequency domain, and thus a time-domain sampling will produce aliasing artifacts. As discussed in [8], the spectral deviation from the original modal transfer function depends on design parameters such as the radius r, spherical harmonic order n, and the sampling frequency f_{s}.

Recently, we proposed an improved radial filter design [10], which was inspired by a virtual analog modeling method [12]. A continuous-time anti-aliasing filter is applied to the modal impulse response by using a polynomial interpolation kernel. This leads to a closed-form expression of a quasi band-limited modal impulse response which can be sampled with reduced aliasing. A considerable improvement in accuracy is thereby achieved without oversampling.

In this paper, we tackle the aliasing problem with an alternative approach which comprises of three steps:

1. Pre-emphasis by taking the antiderivative of the modal impulse response
2. Time-domain sampling of the pre-emphasized impulse response
3. De-emphasis of the sampled signal by using a digital differentiator.

The presented approach was motivated by another virtual analog synthesis method introduced in [13].

In the remainder, the nth-order modal impulse response will be expressed as

$$g_n(t) = \begin{cases} 0, & |\frac{t}{\tau}| > 1 \\ \frac{1}{2\tau}P_n(\frac{t}{\tau}), & |\frac{t}{\tau}| < 1, \end{cases} \qquad (3)$$

where $\tau = \frac{r}{c}$ is the time-of-flight from the origin to $\boldsymbol{x}$. As listed in Table 1 (blue), the nth-order modal impulse response is described by an nth-order polynomial.

Pre-emphasis

The main goal of the pre-emphasis is to reduce the spectral components above the Nyquist frequency ($\frac{f_{\mathrm{s}}}{2}$),

[1] The time harmonic term $e^{i\omega t}$ is omitted.

so that the aliasing artifacts are reduced when the continuous-time signals are sampled. This is carried out analytically by taking the (first-order) antiderivative of the modal impulse response,

$$g_n^{(-1)}(t) \coloneqq \int_{-\infty}^{t} g_n(\tilde{t})\,\mathrm{d}\tilde{t} = \begin{cases} 0, & \frac{t}{\tau} < -1 \\ \frac{1}{2\tau}\int_{-\tau}^{t} P_n(\frac{\tilde{t}}{\tau})\,\mathrm{d}\tilde{t}, & |\frac{t}{\tau}| < 1 \\ \frac{1}{2}\delta_{n0}, & \frac{t}{\tau} > 1, \end{cases} \tag{4}$$

where δ_{nm} denotes the Kronecker delta. For $n \geq 1$, the pre-emphasized modal impulse responses exhibit a finite support in time which are described by $(n+1)$th-order polynomials. For the zeroth order ($n = 0$), however, the antiderivative is a right-sided signal with an infinite length, which cannot be modeled by an FIR filter.

This behavior can be explained in the Laplace domain, where the antiderivative corresponds to a spectral weighting of $\frac{1}{s}$. The dc pole introduced by the antiderivative is canceled out only if the modal transfer function has at least one dc zero. This is the case for $n \geq 1$ as depicted in Fig. 1(b). For $n = 0$, the pre-emphasized radial function exhibits a dc pole which makes it an unstable system. The corresponding impulse response is no longer absolutely integreable [14].

If a stronger pre-emphasis is required, higher-order antiderivatives can be considered. For the same reason as discussed above, the antiderivative order k must be less than or equal to the spherical harmonic order n, since the corresponding Laplace transform is $\frac{1}{s^k}$. The pre-emphasized modal impulse response satisfying $n \geq k$ can be expressed as

$$g_n^{(-k)}(x) = \begin{cases} 0, & |\frac{t}{\tau}| > 1 \\ \frac{\tau^{k-1}}{2^{n+1}n!}\frac{\mathrm{d}^{n-k}}{\mathrm{d}t^{n-k}}\big((\frac{t}{\tau})^2 - 1\big)^n, & |\frac{t}{\tau}| < 1 \end{cases} \tag{5}$$

which follows from the Rodrigues' formula [15, Eq. (14.7.13)]. If $k = n$, which is the maximum allowable antiderivative order for a given modal order n, the time-domain expression (5) reads

$$g_n^{(-n)}(x) = \begin{cases} 0, & |\frac{t}{\tau}| > 1 \\ \frac{\tau^{n-1}}{2^{n+1}n!}\big((\frac{t}{\tau})^2 - 1\big)^n, & |\frac{t}{\tau}| < 1, \end{cases} \tag{6}$$

which can be also found in [16, Eq. (25)–(31)]. In Table 1, the polynomial representations of the antiderivatives are listed for selected n and k.

The temporal and spectral properties of the pre-emphasized modal impulse responses are illustrated in Fig. 1(a) and Fig. 1(b). Note that, at high frequencies ($\frac{\omega}{c}r > n$), the decay rate increases to $(k+1) \times -20\,\mathrm{dB}$/decade irrespective to the modal order n. It can be also seen that higher-order antiderivatives lead to smoother impulse responses at $|\frac{t}{\tau}| = 1$.

Sampling

The pre-emphasized modal impulse responses ($n \leq k$) are uniformly sampled at a given sampling rate f_s. Since only the finite interval $|\frac{t}{\tau}| < 1$ must be considered, the length of the discrete-time sequence is $2\lfloor \tau f_\mathrm{s} \rfloor + 1$ samples. Note that the pre-emphasized spectrum is not ideally band limited. Although reduced, time-domain sampling still produces aliasing artifacts.

De-emphasis

Once the pre-emphasized modal impulse response is sampled, a de-emphasis is applied to restore the original spectrum of the radial function. Ideally, the de-emphasis should have a transfer function of $i\omega$. In this paper, we use an IIR digital differentiator, [17, Eq. (5)],

$$H_\mathrm{diff}(z) = \frac{8}{7T_\mathrm{s}}\frac{1 - z^{-1}}{1 + \frac{1}{7}z^{-1}}. \tag{7}$$

which achieves an accurate magnitude response with moderate phase errors at high frequencies. The resulting group delay is in the order of 10 µs. In order to use the de-emphasized signal as an FIR filter, the output of the IIR differentiator is evaluated only up to a finite length.

Note that the spectral tilting ($\approx i\omega$) introduced by the de-emphasis not only modifies the spectrum of the pre-emphasized modal impulse response but also the aliasing spectrum. The distortion occurring in low frequencies is thereby further reduced at the cost of increased aliasing artifacts at high frequencies.

It is worth mentioning the main difference between the proposed method and the band-limitation approach introduced in [8]. The latter attempts to reduce only the components above the Nyquist limit while keeping the baseband signal unaffected. This is done by employing a continuous-time low-pass filter such as the Lagrange interpolation kernel. No post-processing is thus needed. In the proposed approach, the pre-processing (pre-emphasis) affects the entire frequency range which has to be compensated for in a post-processing (de-emphasis) after the sampling.

Evaluation

In this section, the proposed method is used to build the plane-wave radial filters for radius $r = 0.1\,\mathrm{m}$ and sampling frequency $f_\mathrm{s} = 48\,\mathrm{kHz}$. The speed of sound is set to $c = 343\,\mathrm{m/s}$. We only consider the first-order antiderivatives ($k = 1$) for the pre-emphasis. For each mode, 29 samples are obtained by sampling the pre-emphasized modal impulse response within $|\frac{t}{\tau}| < 1$. The de-emphasis is performed by using the aforementioned IIR differentiator. Thirty-three output samples are used as the FIR coefficients which are depicted in Fig. 2(a). For the zeroth order ($n = 0$), where a pre-emphasis is infeasible, the FIR coefficients are obtained by directly sampling the original modal impulse response.

The magnitude response of each radial filter, shown in Fig. 2(b), is in good agreement with the original spectrum. Compared to direct sampling without pre/post-processing (indicated by thin red line), noticeable improvements are observed in low frequencies. Some devi-

ations can be seen close to the Nyquist frequency which are due to aliasing that are not completely suppressed.

In Fig. 3, a modally band-limited (maximum order $N = 10$) plane wave is simulated and the spectral deviations from the original spectrum are shown for different angular positions ($r = 1\,\mathrm{m}$, $\Theta = 0, \frac{\pi}{2}$). The results are compared for three different radial filter design methods: (i) Direct sampling without pre/post-processing, (ii) band-limitation method using the fifth-order Lagrange interpolator [10], and (iii) the proposed method based on pre/de-emphasis[2]. It can be seen that the band-limitation method achieves a high accuracy for a wide frequency range. Although inferior to the band-limitation method, the proposed approach clearly outperforms direct sampling. Note that the difference between the complex (red) and magnitude (yellow) spectrum errors is more pronounced for the proposed method, which is attributed to the non-ideal phase response of the digital differentiator.

Conclusion

This paper addresses the time-domain modeling of plane-wave radial functions. As an alternative to a recently proposed band-limitation method [10], we presented a novel radial filter design with reduced aliasing artifacts. In the proposed method, the antiderivatives of the modal impulse responses are sampled and post-processed by a digital differentiator which reshapes the spectrum. Since the polynomial coefficients describing the antiderivatives are independent of other design parameters (i.e. radius r, speed of sound c, and sampling rate f_s), they can be pre-computed and reused, which is beneficial for real-time applications. The resulting radial filters exhibit an accurate magnitude spectrum with moderate phase errors at high frequencies. If required, the method can be further improved by employing a more accurate differentiator (e.g. linear-phase FIR filter) or by combining it with the band-limitation method (e.g. with a low-order interpolator). The proposed method is expected to be used for spatial sound reproduction techniques such as wave field synthesis [18].

References

[1] E. G. Williams, *Fourier Acoustics: Sound Radiation and Nearfield Acoustical Holography*. London, UK: Academic Press, 1999.

[2] N. A. Gumerov and R. Duraiswami, *Fast Multipole Methods for the Helmholtz Equation in Three Dimensions*. Oxford, UK: Elsevier, 2005.

[3] J. Ahrens, *Analytic Methods of Sound Field Synthesis*. Berlin, Germany: Springer, 2012.

[4] B. Rafaely, *Fundamentals of Spherical Array Processing*, 2nd ed. Berlin, Germany: Springer, 2019.

[5] H. Pomberger, "Angular and radial directivity control for spherical loudspeaker arrays," Master's thesis, University of Music and Performing Arts, Graz, Austria, 2008.

[6] F. Zotter, "Analysis and synthesis of sound-radiation with spherical arrays," Ph.D. dissertation, University of Music and Performing Arts, Graz, Austria, 2009.

[7] S. Lösler and F. Zotter, "Comprehensive radial filter design for practical higher-order Ambisonic recording," in *Proc. 41st German Annu. Conf. Acoust. (DAGA)*, 2015, pp. 452–455.

[8] N. Hahn, F. Schultz, and S. Spors, "Time domain sampling of the radial functions in spherical harmonics expansions," *IEEE Trans. Signal Process.*, vol. 69, pp. 4502–4512, 2021.

[9] N. Hahn and S. Spors, "Discrete time modeling of spherical harmonics expansion by using band-limited step functions," in *Proc. 46th German Annu. Conf. Acoust. (DAGA)*, Hannover, Germany, Mar. 2020, pp. 1188–1191.

[10] N. Hahn, F. Schultz, and S. Spors, "Higher order antiderivatives of band limited step functions for the design of radial filters in spherical harmonics expansions," in *Proc. 24th Int. Conf. Digital Audio Effects (DAFx)*, Online, Sep. 2021, pp. 184–190.

[11] S. A. Azizoglu, S. S. Koc, and O. M. Buyukdura, "Spherical wave expansion of the time-domain free-space dyadic green's function," *IEEE Trans. Antennas Propag.*, vol. 52, no. 3, pp. 677–683, 2004.

[12] V. Välimäki, J. Pekonen, and J. Nam, "Perceptually informed synthesis of bandlimited classical waveforms using integrated polynomial interpolation," *J. Acoust. Soc. Am. (JASA)*, vol. 131, no. 1, pp. 974–986, 2012.

[13] V. Välimäki, "Discrete-time synthesis of the sawtooth waveform with reduced aliasing," *IEEE Signal Process. Lett.*, vol. 12, no. 3, pp. 214–217, 2005.

[14] B. Girod, R. Rabenstein, and A. Stenger, *Signals and Systems*. Wiley, 2001.

[15] F. W. J. Olver, D. W. Lozier, R. F. Boisvert, and C. W. Clark, *NIST Handbook of Mathematical Functions Handback*. New York, NY, USA: Cambridge University Press, 2010.

[16] S. Bilbao, J. Ahrens, and B. Hamilton, "Incorporating source directivity in wave-based virtual acoustics: Time-domain models and fitting to measured data," *J. Acoust. Soc. Am. (JASA)*, vol. 146, no. 4, pp. 2692–2703, 2019.

[17] M. A. Al-Alaoui, "Novel digital integrator and differentiator," *Electron. Lett.*, vol. 29, no. 4, pp. 376–378, 1993.

[18] N. Hahn, F. Schultz, and S. Spors, "Cylindrical radial filter design with application to local wave field synthesis," *J. Audio Eng. Soc. (JAES)*, in press.

[2] Again, the 0th-order radial filter is designed by direct sampling

Table 1: The antiderivatives of the modal impulse responses $g_n^{(-k)}(x)$. For brevity, the argument is replaced by $x = \frac{c}{r}t$ and the amplitude scaling factor $(\frac{r}{c})^{k-1}$ is omitted. Please also refer to Fig. 1(a).

	$n=0$	$n=1$	$n=2$	$n=3$	$n=4$
$k=0$	$\frac{1}{2}$	$\frac{1}{2}x$	$\frac{3}{4}x^2 - \frac{1}{4}$	$\frac{5}{4}x^3 - \frac{3}{4}x$	$\frac{35}{16}x^4 - \frac{15}{8}x^2 + \frac{4}{3}$
$k=1$		$\frac{1}{4}x^2 - \frac{1}{4}$	$\frac{1}{4}x^3 - \frac{1}{4}x$	$\frac{5}{16}x^4 - \frac{3}{8}x^2 + \frac{1}{16}$	$\frac{7}{16}x^5 - \frac{5}{8}x^3 + \frac{3}{16}x$
$k=2$			$\frac{1}{16}x^4 - \frac{1}{8}x^2 + \frac{1}{16}$	$\frac{1}{16}x^5 - \frac{1}{8}x^3 + \frac{1}{16}x$	$\frac{7}{96}x^6 - \frac{5}{32}x^4 + \frac{3}{32}x^2 - \frac{1}{96}$
$k=3$				$\frac{1}{96}x^6 - \frac{1}{32}x^4 + \frac{1}{32}x^2 - \frac{1}{96}$	$\frac{1}{96}x^7 - \frac{1}{32}x^5 + \frac{1}{32}x^3 - \frac{1}{96}x$
$k=4$					$\frac{1}{768}x^8 - \frac{1}{192}x^6 + \frac{1}{128}x^4 - \frac{1}{192}x^2 + \frac{1}{768}$

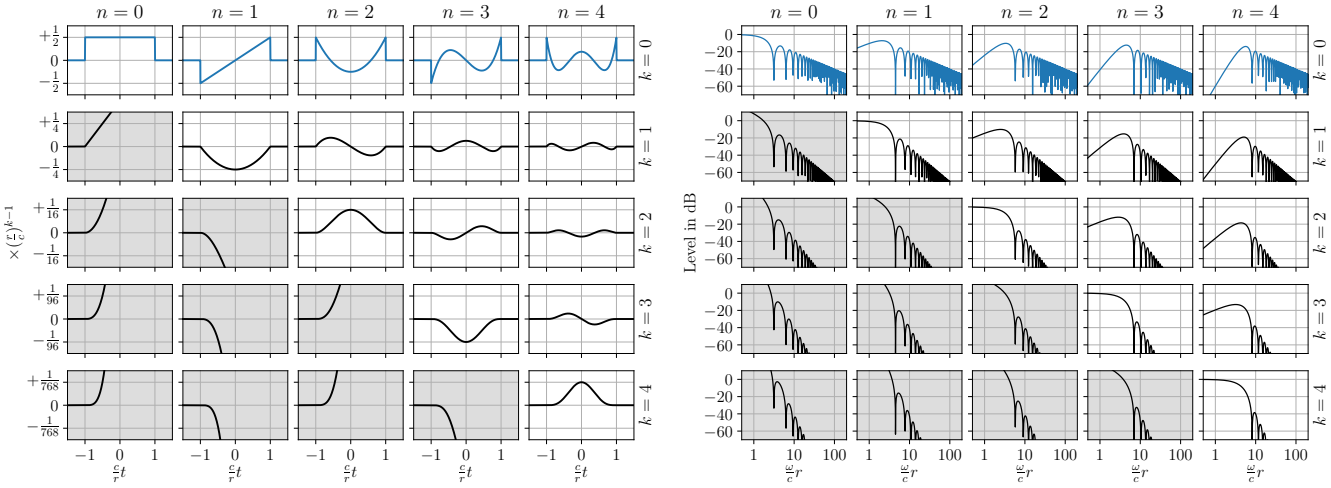

(a) Modal impulse responses **(b)** Modal transfer functions

Figure 1: Pre-emphasized radial functions. The antiderivatives of the modal impulse responses with respect to time t are shown in (a). Please note the scaling factor $(\frac{r}{c})^{k-1}$ indicated in the vertical axis and the different scale in each row. The corresponding transfer functions are shown in (b). For each k, the magnitude responses are normalized by $\frac{(r/c)^k}{(2k+1)!!}$ so that the dc gain for $n = k$ (diagonal) is 0 dB. The shaded subplots ($k > n$) corresponds to the antiderivatives that have an infinite length and thus cannot be be realized as FIR filters.

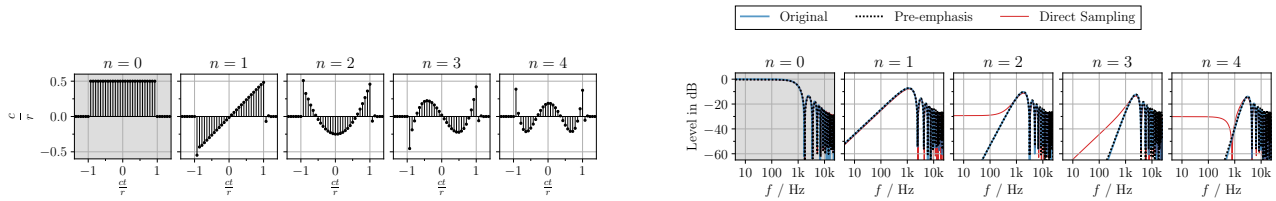

(a) FIR coefficients **(b)** Magnitude responses

Figure 2: Plane-wave radial filters designed by the proposed method (radius $r = 0.1$ m, sampling frequency $f_s = 48$ kHz). The zeroth-order radial filter (shaded) is designed by directly sampling the time-domain representation without pre-empahsis. The FIR coefficients are depicted in (a). The frequency responses (dashed) are compared with the original spectra (blue) in (b). The red curves indicate the results obtained by direct time-domain sampling without pre-/post-processing.

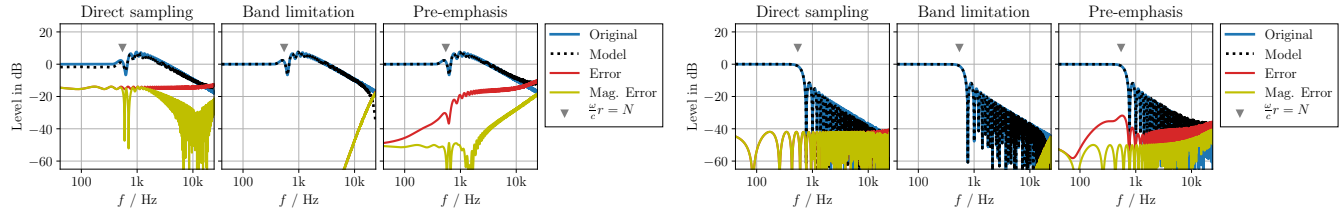

(a) $\Theta = 0$ **(b)** $\Theta = \frac{\pi}{2}$

Figure 3: Discrete-time modeling of a plane wave using different radial filter design methods (modal bandwidth $N = 10$, radius $r = 1$ m, incident angle $\Theta = 0, \frac{\pi}{2}$, sampling frequency $f_s = 48$ kHz).